Synthesis and thermal behavior of $KCe_2(PO_4)_3$, a new full-member in the $A^I M_2^{IV}(PO_4)_3$ family

Taisiya O. Kozlova[1,a], Darya N. Vasilyeva[1,2,b], Daniil A. Kozlov[1,3,c], Mariia A. Teplonogova[1,3,d], Alexander E. Baranchikov[1,e], Nikolay P. Simonenko[1,f], Vladimir K. Ivanov[1,g]

[1]Kurnakov Institute of General and Inorganic Chemistry of the Russian Academy of Sciences, Moscow, Russia
[2]National Research University Higher School of Economics, Moscow, Russia
[3]Lomonosov Moscow State University, Moscow, Russia

[a]taisia.shekunova@yandex.ru, [b]dnvasileva_1@edu.hse.ru, [c]kozlov@inorg.chem.msu.ru,
[d]m.teplonogova@gmail.com,[e]a.baranchikov@yandex.ru, [f]n_simonenko@mail.ru, [g]van@igic.ras.ru

Corresponding author: T. O. Kozlova, taisia.shekunova@yandex.ru

ABSTRACT Hydrothermal treatment of nanoscale amorphous ceric phosphate gel in KOH aqueous solutions was found to result in a new $KCe_2(PO_4)_3$ phase. The refinement of the $KCe_2(PO_4)_3$ structure showed that it was isostructural to recently reported $(NH_4)Ce_2(PO_4)_3$. For the $KCe_2(PO_4)_3$ phase, the unit cell parameters (sp. gr. $C2/c$) were $a = 17.3781(3)$ Å, $b = 6.7287(1)$ Å, $c = 7.9711(2)$ Å, $\beta = 102.351(1)$ °, $V = 910.53(4)$ Å^3, $Z = 4$. The thermal decomposition of $KCe_2(PO_4)_3$ at 800 °C resulted in the mixture of crystalline $CePO_4$ and KPO_3.

1. Introduction

A wide variety of crystalline phosphates of tetravalent metals is mainly represented by double salts [1]. Considerable structural diversity is characteristic of $A^I M_2^{IV}(PO_4)_3$ compounds, which usually belong to the "$NaZr_2(PO_4)_3$" (NASICON) or "$NaTh_2(PO_4)_3$" structural types [2]. The structure of these double phosphates includes a metal-phosphate three-dimensional framework and is characterized by high thermal and chemical stability. Their structural features provide the ability for ion exchange and prospects for their application as matrices for radioactive elements immobilization [3–6], as well as for design of luminescent materials [7–9].

Interestingly, in comparison with actinide phosphates, only 13 crystal structures of ceric phosphates have been reliably characterized until present [10] despite the rich coordination chemistry of Ce(IV) [11] and more than a century of research in ceric phosphates [12]. The lack of information on double cerium(IV) phosphates is primarily due to the high tendency of Ce(IV) to reduce to the trivalent state in the phosphate matrix and form cerium(III) phosphate, which is characterized by extremely high thermodynamic stability [13]. Note that for the compounds having $A^I M_2^{IV}(PO_4)_3$ (where M = Ce^{IV}) composition, only the $NH_4Ce_2(PO_4)_3$ phosphate isostructural to $NH_4Th_2(PO_4)_3$ was reliably characterised [14]. Taking in mind the proximity of the potassium and ammonium ionic radii (1.51 Å [15] and 1.54 Å [16], CN = 8, respectively), the existence of $KCe_2(PO_4)_3$ being an isostructural analog of $NH_4Ce_2(PO_4)_3$ is anticipated. This assumption is also based on the recently reported pairs of isostructural compounds $NH_4Th_2(PO_4)_3$ [17] – $KTh_2(PO_4)_3$ [18], and $K_2Ce(PO_4)_2$ [19] – $K_2Th(PO_4)_2$ [20].

Thus, this work was aimed at the synthesis of $KCe_2(PO_4)_3$ double cerium(IV)-potassium phosphate. The synthesis strategy was based on the hydrothermal treatment of nanoscale ceric phosphate gels. Their chemical composition can easily be adjusted by electrolyte switching and their fibrous ($\sim$ 20 nm) structure makes them highly reactive and prone to crystallisation in aqueous media under relatively mild conditions. This strategy was successfully implemented recently to synthesize new crystalline cerium(IV) phosphates, including $NH_4Ce_2(PO_4)_3$ [14, 21, 22].

2. Experimental Section

The following materials were used as received, without further purification: $Ce(NO_3)_3 \cdot 6H_2O$ (pure grade, Lanhit Russia), potassium hydroxide (pure grade, Sigma Aldrich), phosphoric acid (85 wt.% aq, $\rho = 1.689$ g/cm^3, extra-pure grade, Komponent-Reaktiv Russia), aqueous ammonia (25 wt.%, extra-pure grade, Khimmed Russia), isopropanol (extra-pure grade, Khimmed Russia), distilled water.

First, ceric phosphate solution was synthesized according to the procedure reported earlier [21]. Briefly, nanocrystalline (4 – 5 nm) cerium dioxide (0.100 g) obtained by precipitation from $Ce(NO_3)_3 \cdot 6H_2O$ aqueous solution [23] was dissolved in concentrated phosphoric acid (5 ml) at 80 °C. The calculated molar ratio of Ce:P in the solution was 1:126. To the cooled solution, 35 ml of 1 M potassium hydroxide aqueous solution was added under vigorous stirring. The resulting gel-like precipitate ($\sim$ 40 mL) was placed in 100 ml Teflon autoclave and subjected to hydrothermal treatment at 180 °C for 24 h. After cooling the autoclave, a precipitate was repeatedly washed using distilled water and dried at 60 °C in air.

Powder X-ray diffraction (PXRD) patterns were acquired using a D/MAX 2500 PC (Rigaku, Japan) powder diffractometer with a rotating anode in the reflection geometry (Bragg-Brentano) with Cu K$\alpha_{1,2}$ radiation and a graphite monochromator. PXRD patterns were collected in the 5 – 100 °2θ range with a 0.01 ° step. The identification of the diffraction peaks was carried out using the ICDD database (PDF2, release 2020). PXRD pattern refinement was performed using Rietveld method using the MAUD software [24]. Structure refinement and quantitative phase analysis were carried out using structures of monazite (sp. gr. $P12_1/n1$, $a = 6.788$ Å, $b = 7.0163$ Å, $c = 6.465$ Å, $\beta = 103.43°$, $V = 299.486$ Å^3, $Z = 4$) [25] and KPO$_3$ (sp. gr. $P12_1/a1$, $a = 14.02$ Å, $b = 4.54$ Å, $c = 10.28$ Å, $\beta = 101.5°$ $V = 641.194$ Å^3, $Z = 8$) [26] taken from Crystallography Open Database [27].

Scanning electron microscopy (SEM) images were obtained using an Amber GMH (Tescan, Czech Republic) microscope operated at an accelerating voltage of 5 kV using a secondary electron (Everhart–Thornley) and backscattered electron (Low Energy BSE) detectors. Energy-dispersive X-ray spectroscopy (EDS) was performed using an Ultim Max (Oxford Instruments, UK) detector at an accelerating voltage of 20 kV.

The Fourier transform infrared (FT-IR) spectra of the samples were recorded using a Bruker ALPHA spectrometer in the range of 400 – 4000 cm^{-1} in attenuated total reflectance mode.

3. Results and discussion

According to powder X-ray diffraction data, hydrothermal treatment of ceric phosphate gel resulted in the formation of a crystalline product with a diffraction pattern similar to $NH_4Ce_2(PO_4)_3$ phase (monoclinic, sp. gr. $C2/c$, $a = 17.4719(4)$ Å, $b = 6.76928(14)$ Å, $c = 7.99286(14)$ Å, $\beta = 102.873(1)°$, $V = 921.57(4)$ Å^3, $Z = 4$) [14]. According to EDS analysis, the average K:Ce:P atomic ratio was close to 1:2:3, which corresponds to the nominal composition of $KCe_2(PO_4)_3$. PXRD pattern of the obtained sample showed that it is contained an admixture of $CePO_4$ with monazite structure (PDF2 [00-032-199]), so further refinement of the structure was carried out taking into account the two-phase composition of the powder. Crystal structure refinement by the Rietveld method was performed using the MAUD software. Experimental and calculated PXRD patterns are shown in Fig. 1. Despite the fact that the measured diffraction pattern corresponded well to the calculated one, the refinement was characterized by rather large R-factor values ($R_p = 0.087$, $R_{wp} = 0.13$), which may be caused by unaccounted structural deviations or the presence of water molecules in the channels of cerium(IV)-potassium phosphate structure. The $KCe_2(PO_4)_3$ phase, similarly to its ammonium analogue, crystallizes in a monoclinic crystal system (sp. gr. $C2/c$, $a = 17.3781(3)$ Å, $b = 6.7287(1)$ Å, $C = 7.9711(2)$ Å, $\beta = 102.351(1)°$, $V = 910.53(4)$ Å^3, $Z = 4$).

The structure of the resulting cerium(IV)-potassium phosphate is shown in Fig. 2. The coordination number of cerium in this structure was 9, Ce is surrounded by oxygen atoms of phosphate groups, while the potassium cations are arranged in channels along the c axis. Note that the $CePO_4$ content in the initial sample determined by quantitative phase analysis is rather small and amounts to 3.1 ± 0.1 wt. %. The formation of cerium(III) phosphate upon hydrothermal treatment of ceric phosphate gels is rather unusual. This fact along with the similar report [21] can contribute to one of the most disputable topics of the chemistry of nanocrystalline ceria, namely its oxygen non-stoichiometry [28–30]. The possibility of the partial reduction of Ce(IV) during hydrothermal synthesis of crystalline cerium(IV) phosphates, as well as monazite structure formation under hydrothermal conditions, have been also discussed recently [31–34] but the exact mechanisms were not analyzed in detail and require further studies.

The newly synthesized double ceric phosphate $KCe_2(PO_4)_3$ complements the family of isostructural compounds having the composition of $A^I M_2^{IV}(PO_4)_3$ (A^I =Li, Na, K, NH$_4$, M^{IV} = Th, U) [17, 18, 35–37]. Note that the synthesis of the "$KCe_2(PO_4)_3$" with a monazite structure was recently announced [38]. However, this announcement is doubtful due to the absence of the structural data. Moreover, at the temperatures (above 600 °C) used to synthesize this compound [38], cerium(IV) is extremely prone to reduction to trivalent state [34, 39, 40]. Similarly, the previously reported synthesis of $BaCe(PO_4)_2$ [38] was further argued [41].
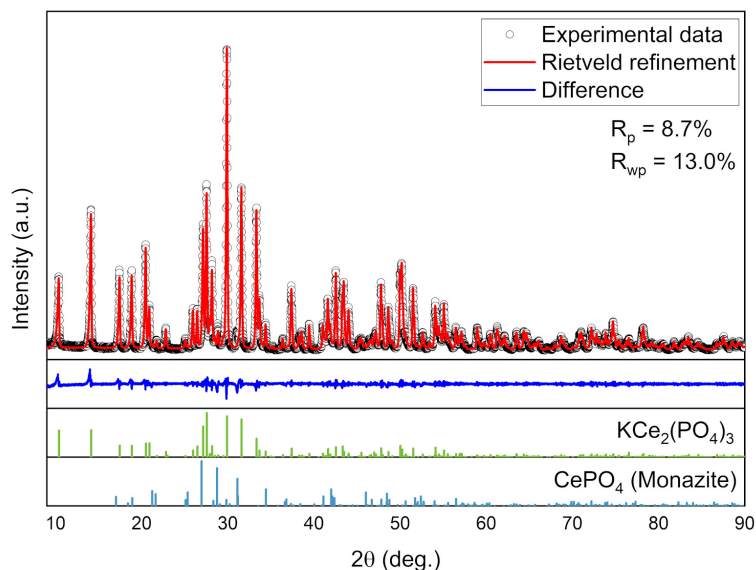
FIG. 1. Rietveld plot for the powder obtained upon hydrothermal treatment of ceric phosphate gel (observed, calculated and difference PXRD profiles along with Bragg peak positions)
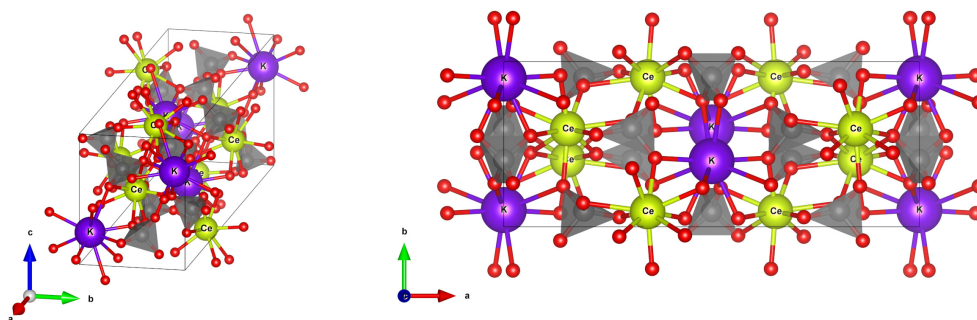
FIG. 2. Crystal structure of $KCe_2(PO_4)_3$. Yellow spheres denote Ce atoms, K atoms are shown in violet, O atoms are presented as red spheres, P atoms are located in PO_4 tetrahedra (shown in gray)

The comparison of thermal behavior of isostructural $NH_4Ce_2(PO_4)_3$ and $KCe_2(PO_4)_3$ compounds is quite interesting since the formation of single-phase cerium(III) orthophosphate with monazite structure during $NH_4Ce_2(PO_4)_3$ thermolysis was previously observed [14]. On the other hand, the thermolysis of $K_2Ce(PO_4)_2$ cerium(IV)-potassium phosphate above 850 °C resulted in the formation of $K_3Ce(PO_4)_2$ cerium(III)-potassium phosphate as well as of $CePO_4$ [19].

According to the thermal analysis, the thermolysis of $KCe_2(PO_4)_3$ (with an admixture of *ca.* 3.1 ± 0.1 wt. % $CePO_4$) proceeds in two main stages (Fig. 3). The first stage begins at $\sim$220 °C and ends at 540 °C and is apparently associated with the release of water (probably presented in the channels of the $KCe_2(PO_4)_3$ structure) as well as oxygen [10, 42]. The second stage begins at about 600 °C and corresponds to the release of oxygen due to the reduction of cerium(IV) to cerium(III).

To clarify the processes occurring at each stage of thermal decomposition of $KCe_2(PO_4)_3$ and to estimate the composition of the thermolysis products, the synthesized $KCe_2(PO_4)_3$ (with 3.1 ± 0.1 wt. % $CePO_4$ admixture) was annealed at either 580 °C or 800 °C in a muffle furnace for 2 h in air (the heating rate was 5 °C/min).

Quantitative phase analysis of PXRD data showed that the heating at 580 °C did not change dramatically the phase composition of the powder. Like the bare sample, it contained $KCe_2(PO_4)_3$ as the major component and an admixture of $CePO_4$ (23 ± 5 wt. %). The reduction of cerium(IV) to cerium(III) at high temperatures is characteristic of tetravalent cerium phosphates and has been repeatedly observed recently [14, 19, 43, 44].

According to PXRD, the thermal treatment of $KCe_2(PO_4)_3$ at 800 °C resulted in its complete decomposition and the formation of $CePO_4$ and potassium polyphosphate KPO_3 (PDF2 35-819). According to quantitative phase analysis, the content of KPO_3 in the product was 21.0 ± 1.2 wt. % (34.6 ± 2.0 mol. %), which agreed well with the anticipated molar ratio $CePO_4$:$KPO_3 = 2$:1. Thus, the thermolysis of $KCe_2(PO_4)_3$ in air can be described by the following reaction scheme:

$$KCe_2(PO_4)_3 \rightarrow 2CePO_4 + KPO_3 + \frac{1}{2}O_2 \uparrow . \tag{1}$$
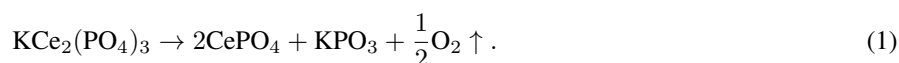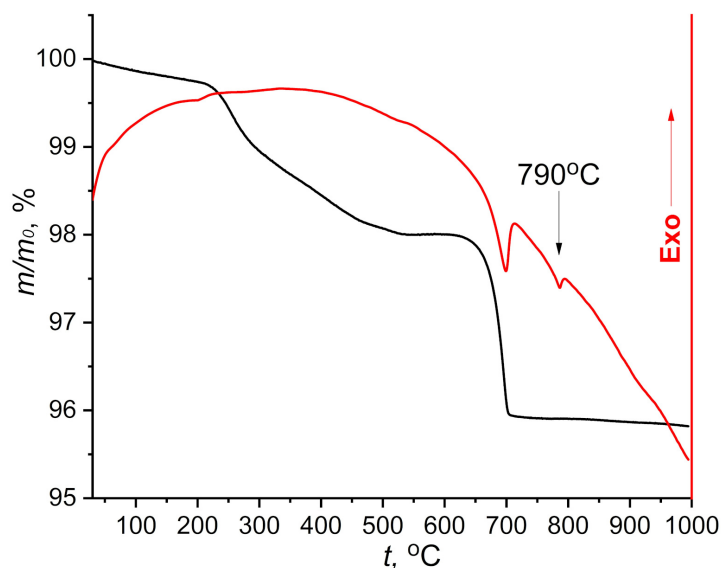
FIG. 3. Thermal decomposition curve of KCe$_2$(PO$_4$)$_3$ (with 3.1 ± 0.1 wt. % CePO$_4$ admixture) in air

In accordance with eqaution (1), the total weight loss for the KCe$_2$(PO$_4$)$_3$ phase should be *ca.* 2.5 wt. %, whereas the experimentally measured weight loss was much greater ($\sim$ 4 wt. %). Such a difference can be due to the presence of water molecules in the structure of KCe$_2$(PO$_4$)$_3$ which were not accounted during the structural analysis. These H$_2$O molecules can be trapped in the KCe$_2$(PO$_4$)$_3$ structural channels and release from the phase at temperatures up to 540 °C. Our estimates of the water content resulted in the chemical composition of KCe$_2$(PO$_4$)$_3 \cdot$ 0.4H$_2$O. Most probable, the water content can vary in a certain range and the exact chemical composition of KCe$_2$(PO$_4$)$_3 \cdot x$H$_2$O needs further refinement.
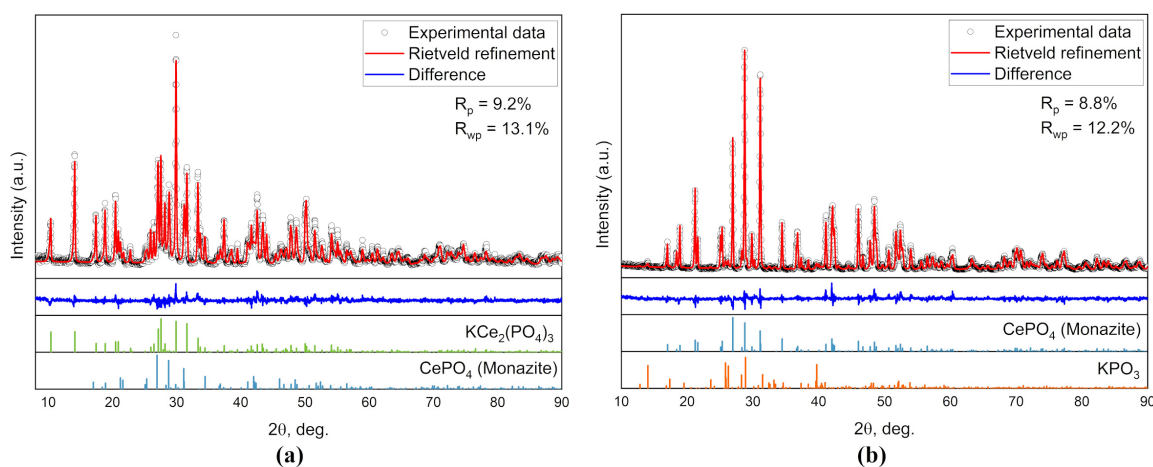
FIG. 4. Rietveld plots for the samples obtained after the thermal treatment of KCe$_2$(PO$_4$)$_3$ (with 3.1 ± 0.1 wt. % CePO$_4$ admixture) sample at 580 °C (a) or 800 °C (b) (observed, calculated and difference PXRD profiles along with Bragg peaks positions for CePO$_4$ and KPO$_3$)

Figure 5 shows the IR spectra of the bare KCe$_2$(PO$_4$)$_3$ sample (with 3.1 ± 0.1 wt. % CePO$_4$ admixture) and the samples obtained after its thermal treatment at 580 °C or 800 °C. The IR spectra for the samples before and after the thermal treatment at 580 °C are almost identical and coincide well with the IR spectrum of the NH$_4$Ce$_2$(PO$_4$)$_3$ phase [14]. In the regions of 1100 $-$ 900 cm^{-1} and 650 $-$ 440 cm^{-1} the characteristic absorption bands are observed, which are related to the stretching and bending vibrations of phosphate anions, respectively [33,45].

In the infrared spectrum of the powder obtained at 800 °C, extra absorption bands are presented at 1280 cm^{-1}, 865 cm^{-1}, 760 cm^{-1}, 680 cm^{-1}, and 490 cm^{-1} which correspond to polyphosphate moieties [46–49]. Thus, IR data agree well with the XRD results and confirm the formation of potassium polyphosphate KPO$_3$ upon the thermolysis of cerium(IV)-potassium phosphate KCe$_2$(PO$_4$)$_3$.

According to scanning electron microscopy, the KCe$_2$(PO$_4$)$_3$ phase is represented by 200 nm particles having the shape of truncated octahedrons. Thermal treatment at 580 °C does not significantly change the size of the particles, but after the treatment at 800 °C, large crystals up to several tens of micrometers in size are observed along with the relatively
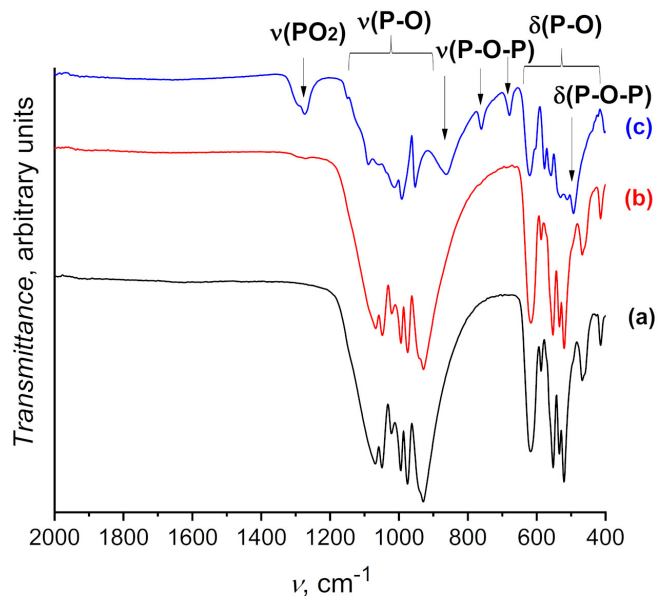
FIG. 5. IR spectra for the samples obtained after the thermolysis of $KCe_2(PO_4)_3$ (with 3.1 ± 0.1 wt. % $CePO_4$ admixture) (a) at $580°C$ (b) or $800°C$ (c)

(a)

(b)

(c)
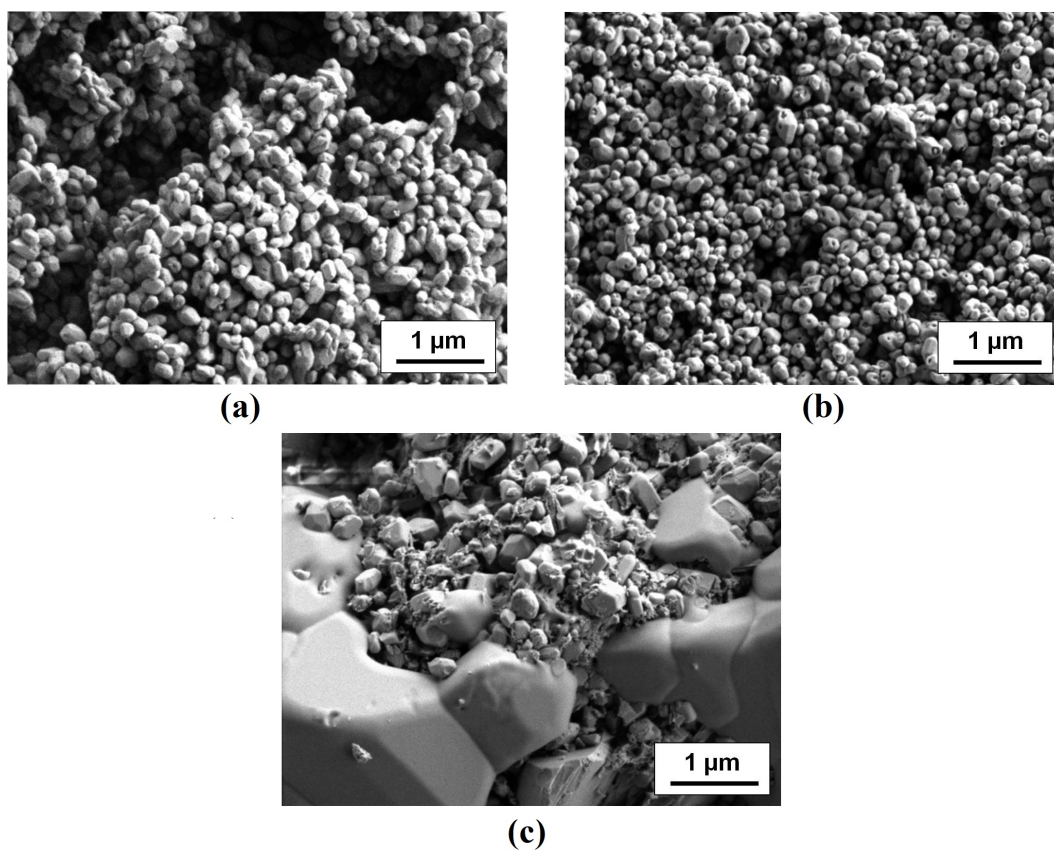
FIG. 6. SEM images for the samples obtained by thermolysis of the bare cerium(IV)-potassium phosphate (a) at $580\ °C$ (b) or $800\ °C$ (c)
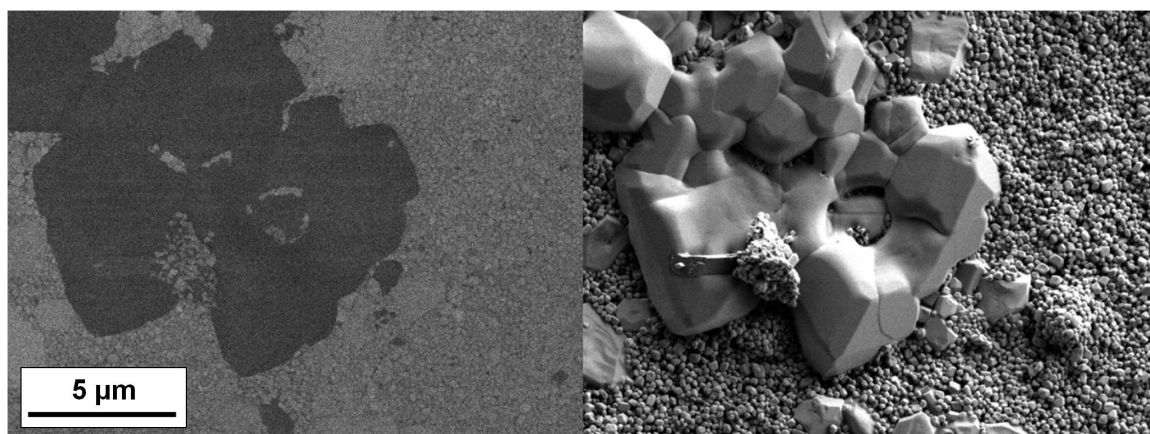
FIG. 7. SEM images for the sample obtained by thermolysis of the bare cerium(IV)-potassium phosphate at 800 °C: backscattered electron detection mode (left), secondary electrons detection mode (right)
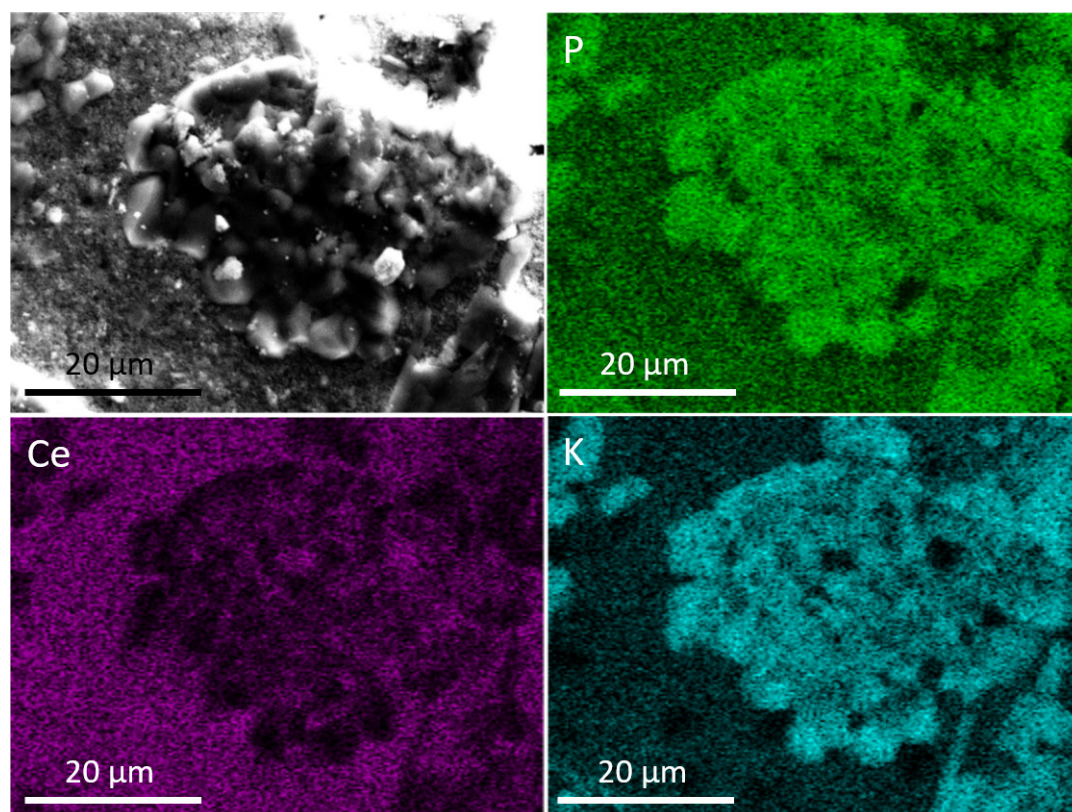
FIG. 8. SEM image and the corresponding EDS distribution maps of P, Ce and K for the sample obtained by thermolysis of the bare cerium(IV)-potassium phosphate at 800 °C

small particles (Fig. 6). The images taken in the backscattered electron detection mode (Fig. 7) show that these large crystals have a lower average atomic weight than the smaller crystals. Thus, it can be assumed that small and large crystals correspond to CePO$_4$ and KPO$_3$ phases, respectively (Fig. 6,7).

Large size of KPO$_3$ crystals is most probably related to their growth from melt which can form upon heating and thermolysis of KCe$_2$(PO$_4$)$_3$. In the CePO$_4$–KPO$_3$–Ce(PO$_3$)$_3$ system [50], the CePO$_4$–KPO$_3$ quasi-binary section corresponds to an eutectic type system with an eutectic point of 790 °C (85 wt. % KPO$_3$). Note, the eutectic point agrees the position of the endothermic effect in the differential scanning calorimetry data for the bare cerium(IV)-potassium phosphate (Fig. 3). Thus, upon its heating to 800 °C, the liquid KPO$_3$-rich phase forms and, upon the subsequent cooling of the two-phase liquid-solid system, the crystallization of potassium polyphosphate occurs. Cerium(III) orthophosphate is anticipated to possess low solubility in the phosphate melt and the size of CePO$_4$ crystals does not change significantly.

The EDS results corroborate the above considerations and indicate that the large aggregates dominantly contain potassium and phosphorus (Fig. 8).

4. Conclusions

In this paper, nanoscale amorphous ceric phosphate was used as a convenient starting material for the hydrothermal synthesis of crystalline ceric phosphates. We have demonstrated that the hydrothermal treatment of the gels obtained by mixing of the ceric phosphate solution and 1 M potassium hydroxide aqueous solution results in the formation of the previously unknown cerium(IV)-potassium phosphate, $KCe_2(PO_4)_3$. $KCe_2(PO_4)_3$ was found to be isostructural to $NH_4Ce_2(PO_4)_3$, and belongs to the $A^I M_2^{IV}(PO_4)_3$ (A^I =Li, Na, K, NH_4, M^{IV} = Th, U) family. Thermal analysis data indicated that double ceric phosphate $KCe_2(PO_4)_3$ decomposes through two stages with the formation of the mixture of $CePO_4$ and KPO_3 at 800 °C.

References

[1] Pet'kov V.I. Complex phosphates formed by metal cations in oxidation states I and IV. *Russ. Chem. Rev.*, 2012, **81**, P. 606–637.

[2] Locock A.J. Crystal chemistry of actinide phosphates and arsenates. *Struct. Chem. Inorg. Actin. Compd.*, Elsevier, Amsterdam, 2007, P. 217–278.

[3] Dacheux N., Clavier N., Robisson A.C., Terra O., Audubert F., Lartigue J.É., Guy C. Immobilisation of actinides in phosphate matrices. *Comptes Rendus Chim.*, 2004, **7**, P. 1141–1152.

[4] Neumeier S., Arinicheva Y., Ji Y., Heuser, Julia M. Kowalski P.M., Kegler P., Schlenz H., Bosbach D., Deissmann G. New insights into phosphate based materials for the immobilisation of actinides. *Radiochim. Acta.*, 2017, **105**, P. 961–984.

[5] Orlova A.I., Kitaev D.B., Volkov Yu.F., Pet'kov V.I., Kurazhkovskaya V.S., Spiridonova M.L. Double phosphates of Ce(IV) and some mono- and bivalent elements. *Radiochemistry*, 2001, **43**, P. 225–228.

[6] Achary S.N., Bevara S., Tyagi A.K. Recent progress on synthesis and structural aspects of rare-earth phosphates. *Coord. Chem. Rev.*, 2017, **340**, P. 266–297.

[7] Asabina E., Sedov V., Pet'kov V., Deyneko D., Kovalsky A. Synthesis, structure and luminescence properties of the europium–containing NASI-CON type phosphates. *J. Sol-Gel Sci. Technol.*, 2023.

[8] Krutyak N., Spassky D., Deyneko D.V., Antropov A., Morozov V.A., Lazoryak B.I., Nagirnyi V. NASICON-type $Na_{3.6}Lu_{1.8-x}(PO_4)_3:xEu^{3+}$ phosphors: Structure and luminescence. *Dalt. Trans.*, 2022, **51**, P. 11840–11850.

[9] Kozlova T.O., Popov A.L., Kolesnik I.V., Kolmanovich D.D., Baranchikov A.E., Shcherbakov A.B., Ivanov V.K. Amorphous and crystalline cerium(IV) phosphates: Biocompatible ROS-scavenging sunscreens. *J. Mater. Chem. B.*, 2022, **10**, P. 1775–1785.

[10] Kozlova T.O., Baranchikov A.E., Ivanov V.K. Cerium(IV) orthophosphates (Review). *Russ. J. Inorg. Chem.*, 2021, **66**, P. 1761–1778.

[11] So Y.M., Leung W.H. Recent advances in the coordination chemistry of cerium(IV) complexes. *Coord. Chem. Rev.*, 2017, **340**, P. 172–197.

[12] Hartley W.N. Contributions to the chemistry of cerium compounds. *J. Chem. Soc. Trans.*, 1882, **41**, P. 202–209.

[13] Sroor F.M.A., Edelmannand F.T. Tetravalent chemistry: Inorganic. *Rare Earth Elem. Fundam. Appl.*, John Wiley & Sons Ltd, Chichester, 2012, P. 313–320.

[14] Shekunova T.O., Istomin S.Y., Mironov A.V., Baranchikov A.E., Yapryntsev A.D., Galstyan A.A., Simonenko N.P., Gippius A.A., Zhurenko S.V., Shatalova T.B., Skogareva L.S., Ivanov V.K. Crystallization pathways of cerium(IV) phosphates under hydrothermal conditions: A search for new phases with a tunnel structure. *Eur. J. Inorg. Chem.*, 2019, **27**, P. 3242–3248.

[15] Shannon R.D., Prewitt C.T. Effective ionic radii in oxides and fluorides. *Acta Crystallogr. Sect. B Struct. Crystallogr. Cryst. Chem.*, 1969, **25**, P. 925–946.

[16] Sidey V. On the effective ionic radii for ammonium. *Acta Crystallogr. Sect. B Struct. Sci. Cryst. Eng. Mater.*, 2016, **72**, P. 626–633.

[17] Salvadó M.A., Pertierra P., Bortun A.I., Trobajo C., Garcia J.R. Phosphorous acid and urea: Valuable sources of phosphorus and nitrogen in the hydrothermal synthesis of ammonium-thorium phosphates. *Inorg. Chem.*, 2008, **47**, P. 7207–7210.

[18] Matkovic B., Prodic B., Sljukic M. The crystal structure of potassium dithorium trisphosphate, $KTh_2(PO_4)_3$. *Croat. Chem. Acta.*, 1968, **40**, P. 147.

[19] Bevara S., Achary S.N., Patwe S.J., Sinha A.K., Tyagi A.K. Preparation and crystal structure of $K_2Ce(PO_4)_2$: A new complex phosphate of Ce(IV) having structure with one-dimensional channels. *Dalt. Trans.*, 2016, **45**, P. 980–991.

[20] Yu N., Klepov V.V., Schlenz H., Bosbach D., Kowalski P.M., Li Y., Alekseev E.V. Cation-dependent structural evolution in $A_2Th(T^V O_4)_2$ (A = Li, Na, K, Rb, Cs; T = P and As) series. *Cryst. Growth Des.*, 2017, **17**, P. 1339–1346.

[21] Shekunova T.O., Baranchikov A.E., Ivanova O.S., Skogareva L.S., Simonenko N.P., Karavanova Yu. A., Lebedev V.A., Borilo L.P., Ivanov V.K. Cerous phosphate gels: Synthesis, thermal decomposition and hydrothermal crystallization paths. *J. Non. Cryst. Solids.*, 2016, **447**, P. 183–189.

[22] Kozlova T.O., Mironov A.V., Istomin S.Y., Birichevskaya K.V., Gippius A.A., Zhurenko S.V., Shatalova T.B., Baranchikov A.E., Ivanov V.K. Meet the cerium(IV) phosphate sisters: $Ce^{IV}(OH)PO_4$ and $Ce_2^{IV}O(PO_4)_2$. *Chem. – A Eur. J.*, 2020, **26**, P. 12188–12193.

[23] Kolesnik I.V., Shcherbakov A.B., Kozlova T.O., Kozlov D.A., Ivanov V.K. Comparative analysis of sun protection characteristics of nanocrystalline cerium dioxide. *Russ. J. Inorg. Chem.*, 2020, **65**, P. 960–966.

[24] Lutterotti L. Total pattern fitting for the combined size–strain–stress–texture determination in thin film diffraction. *Nucl. Instruments Methods Phys. Res. Sect. B Beam Interact. with Mater. Atoms.*, 2010, **268**, P. 334–340.

[25] Ni Y., Hughes J.M., Mariano A.N. Crystal chemistry of the monazite and xenotime structures. *Am. Mineral.*, 1995, **80**, P. 21–26.

[26] Jost K.H., Schulze H.J. Zur phasentransformation des kaliumpolyphosphates $(KPO_3)_x$. *Acta Crystallogr. Sect. B Struct. Crystallogr. Cryst. Chem.*, 1969, **25**, P. 1110–1118.

[27] Graulis S., Chateigner D., Downs R.T., Yokochi A.F.T., Quirós M., Lutterotti L., Manakova E., Butkus J., Moeck P., Le Bail A. Crystallography Open Database – An open-access collection of crystal structures. *J. Appl. Crystallogr.*, 2009, **42**, P. 726–729.

[28] Shcherbakov A.B., Zholobak N.M., Ivanov V.K. Biological, biomedical and pharmaceutical applications of cerium oxide. *Cerium Oxide (CeO2): Synthesis, Properties and Applications*, 2020, Elsevier, Amsterdam, P. 279–358.

[29] Plakhova T.V., Romanchuk A.Y., Yakunin S.N., Dumas T., Demir S., Wang S., Minasian S.G., Shuh D.K., Tyliszczak T., Shiryaev A.A., Egorov A.V., Ivanov V.K., Kalmykov S.N. Solubility of Nanocrystalline Cerium Dioxide: Experimental Data and Thermodynamic Modeling. *J. Phys. Chem. C*, 2016, **120**(39), P. 22615–22626.

[30] Baranchikov A.E., Polezhaeva O.S., Ivanov V.K., Tretyakov Y.D. Lattice expansion and oxygen non-stoichiometry of nanocrystalline ceria. *Cryst EngComm*, 2010, **12**(11), P. 3531–3533.

[31] Enikeeva M.O., Proskurina O.V., Danilovich D.P., Gusarov V.V. Formation of nanocrystals based on equimolar mixture of lanthanum and yttrium orthophosphates under microwave-assisted hydrothermal synthesis. *Nanosyst.: Phys. Chem. Math.*, 2020, **11**(6), P. 705–715.

[32] Kozlova T.O., Vasil'eva D.N., Kozlov D.A., Teplonogova M.A., Birichevskaya K.V., Baranchikov A.E., Gavrikov A.V., Ivanov V.K. On the chemical stability of Ce^{IV}(PO$_4$)(HPO$_4$)$_{0.5}$(H$_2$O)$_{0.5}$ in alkaline media. *Russ. J. Inorg. Chem.*, 2022, **67**, P. 1901–1907.

[33] Skogareva L.S., Shekunova T.O., Baranchikov A.E., Yapryntsev A.D., Sadovnikov A.A., Ryumin M.A., Minaeva N.A., Ivanov V.K. Synthesis of cerium orthophosphates with monazite and rhabdophane structure from phosphoric acid solutions in the presence of hydrogen peroxide. *Russ. J. Inorg. Chem.*, 2016, **61**, P. 1219–1224.

[34] Brandel V., Clavier N., Dacheux N. Synthesis and characterization of uranium (IV) phosphate-hydrogenphosphate hydrate and cerium (IV) phosphate-hydrogenphosphate hydrate. *J. Solid State Chem.*, 2005, **178**, P. 1054–1063.

[35] Topić M., Napijalo M., Popović S. Zeljić Z. Temperature Dependence of Some Properties of NaTh$_2$(PO$_4$)$_3$ Ferroelectric Crystals. *Phys. stat. sol.*, 1972, **11**, P. 787–790.

[36] Guesdon A., Provost J., Ravcau B. New thorium and uranium monophosphates in the KTh$_2$(PO$_4$)$_3$ family: Structure and cationic non-stoichiometry. *J. Mater. Chem.*, 1999, **9**, P. 2583–2587.

[37] Brandel V., Dacheux N. Chemistry of tetravalent actinide phosphates – Part II. *J. Solid State Chem.*, 2004, **177**, P. 4755–4767.

[38] Orlova A.I., Kitaev D.B., Kazantsev N.G., Samoilov S.G. Double phosphates of Ce (IV) and some mono- and divalent elements: synthesis and crystal structure. *Radiochemistry*, 2002, **44**, P. 326–331.

[39] Bregiroux D., Terra O., Audubert F., Dacheux N., Serin V., Podor R., Bernache-Assollant D. Solid-state synthesis of monazite-type compounds containing tetravalent elements. *Inorg. Chem.*, 2007, **46**, P. 10372–10382.

[40] Bamberger C.E., Begun G.M., Brynestad J., Land J.F. Simultaneous precipitation of phosphates of Bi (III) and Ce(IV) or Ce (III). Characterization of precipitates and their ignition products. *Radiochim. Acta.*, 1982, **31**, P. 57–64.

[41] Popa K., Bregiroux D., Konings R.J.M., Gouder T., Popa A.F., Geisler T., Raison P.E. The chemistry of the phosphates of barium and tetravalent cations in the 1:1 stoichiometry. *J. Solid State Chem.*, 2007, **180**, P. 2346–2355.

[42] Kozlova T.O., Baranchikov A.E., Birichevskaya K.V., Kozlov D., Simonenko N.P., Gavrikov A.V., Teplonogova M.A., Ivanov V.K. On the thermal decomposition of cerium(IV) hydrogen phosphate Ce(PO$_4$)(HPO$_4$)$_{0.5}$(H$_2$O)$_{0.5}$. *Russ. J. Inorg. Chem.*, 2021, **66**, P. 1624–1632.

[43] Dacheux N., Podor R., Brandel V., Genet M. Investigations of systems ThO$_2$–MO$_2$–P$_2$O$_5$ (M = U, Ce, Zr, Pu). Solid solutions of thorium-uranium (IV) and thorium-plutonium (IV) phosphate-diphosphates. *J. Nucl. Mater.*, 1998, **252**, P. 179–186.

[44] Bevara S., Mishra K.K., Patwe S.J., Ravindran T.R., Gupta M.K., Mittal R.K., P.S. Ram, Sinha A.K., Achary S.N., Tyagi A.K. Phase transformation, vibrational and electronic properties of K$_2$Ce(PO$_4$)$_2$: A combined experimental and theoretical study. *Inorg. Chem.*, 2017, **56**, P. 3335–3348.

[45] Clavier N., Mesbah A., Szenknect S., Dacheux N. Monazite, rhabdophane, xenotime & churchite: Vibrational spectroscopy of gadolinium phosphate polymorphs. *Spectrochim. Acta – Part A Mol. Biomol. Spectrosc.*, 2008, **205**, P. 85–94.

[46] Jerroudi M., Bih L., Azrour M., Manoun B., Saadoune I., Lazor P. Investigation of novel low melting phosphate glasses inside the Na$_2$O–K$_2$O–ZnO–P$_2$O$_5$ system. *J. Inorg. Organomet. Polym. Mater.*, 2020, **30**, P. 532–542.

[47] Nassar A.M., El Oker M.M., Radwan S.N., Nabhan E. Effect of MO (CuO, ZnO, and CdO) on the compaction of sodium meta phosphate sealing glass. *Curr. Sci. Int.*, 2013, **2**, P. 1–7.

[48] Nabhan E., Abd-Allah W.M., Ezz-El-Din F.M. Optical study of gamma irradiated sodium metaphosphate glasses containing divalent metal oxide MO (ZnO or CdO). *Results Phys.*, 2017, **7**, P. 119–125.

[49] Ghoneim N.A., Abdelghany A.M., Abo-Naf S.M., Moustafa F.A., Elbadry Kh.M. Spectroscopic studies of lithium phosphate, lead phosphate and zinc phosphate glasses containing TiO$_2$: Effect of gamma irradiation. *J. Mol. Struct.*, 2013, **1035**, P. 209–217.

[50] Szczygiel I. The system CePO$_4$-KPO$_3$-Ce(PO$_3$)$_3$. *Thermochim. Acta.*, 2003, **402**, P. 153–158.

Information about the authors:

T. O. Kozlova – Kurnakov Institute of General and Inorganic Chemistry of the Russian Academy of Sciences, Leninsky prospect, 31, Moscow, 119991, Russia; ORCID 0000-0002-9757-9148; taisia.shekunova@yandex.ru

D. N. Vasilyeva – Kurnakov Institute of General and Inorganic Chemistry of the Russian Academy of Sciences, Leninsky prospect, 31, Moscow, 119991, Russia; National Research University Higher School of Economics, Moscow, Myasnitskaya str., 20, 101000, Russia; dnvasileva_1@edu.hse.ru

D. A. Kozlov – Kurnakov Institute of General and Inorganic Chemistry of the Russian Academy of Sciences, Leninsky prospect, 31, Moscow, 119991, Russia; Lomonosov Moscow State University, Leninskie Gory 1, Moscow, 119991, Russia; ORCID 0000-0003-0620-8016; kozlov@inorg.chem.msu.ru

M. A. Teplonogova – Kurnakov Institute of General and Inorganic Chemistry of the Russian Academy of Sciences, Leninsky prospect, 31, Moscow, 119991, Russia; Lomonosov Moscow State University, Leninskie Gory 1, Moscow, 119991, Russia; ORCID 0000-0002-4820-8498; m.teplonogova@gmail.com

A. E. Baranchikov – Kurnakov Institute of General and Inorganic Chemistry of the Russian Academy of Sciences, Leninsky prospect, 31, Moscow, 119991, Russia; ORCID 0000-0002-2378-7446; a.baranchikov@yandex.ru

N. P. Simonenko – Kurnakov Institute of General and Inorganic Chemistry of the Russian Academy of Sciences, Leninsky prospect, 31, Moscow, 119991, Russia; ORCID 0000-0002-4209-6034; n_simonenko@mail.ru

V. K. Ivanov – Kurnakov Institute of General and Inorganic Chemistry of the Russian Academy of Sciences, Leninsky prospect, 31, Moscow, 119991, Russia; ORCID 0000-0003-2343-2140; van@igic.ras.ru

Conflict of interest: the authors declare no conflict of interest.